CHAPTER V
A NOVEL SOFT AND COTTON-LIKE CHITOSAN-SUGAR NANOSCAFFOLD

Abstract

A novel type of chitosan nanoscaffold with a soft and cotton-like appearance is proposed. The key to the success is based on two points: (i) the change in morphology of chitin whisker to chitosan nanoscaffold and (ii) the surface modification of the nanoscaffold chitosan with a sugar unit. Simple deacetylation of chitin whisker gives a colloidal solution of chitosan, of which the chitosan is in a nanoscaled scaffold. Surface functionalization of the chitosan nanoscaffold with lactose or maltose via a heterogeneous system in water at room temperature results in a soft and cotton-like chitosan containing mesopores. As all steps are organic solvent free, this chitosan-sugar nanoscaffold might be a promising material for biopolymer-supported tissue engineering.

Keywords: chitin; whisker; chitosan; nanoscaffold; tissue engineering; lactose; maltose

Introduction

Chitin-chitosan is a naturally occurring copolymer of β-(1-4)-2-acetamido-2-deoxy-β-D-glucose and β-(1-4)-2-amino-2-deoxy-β-D-glucose obtained from the shells of crustaceans, cuticles of insects, and cell walls of fungi and yeasts. The copolymer exhibits specific properties, especially bioactivity,[1] biocompatibility,[2] biodegradability,[3] and non-toxicity[4] to afford the potential applications in pharmaceutical and biomedical fields. In the past, simple materializations, such as solvent casting for films,[5] spray drying for beads or spheres,[6] and cross-linking for gels or membranes[7] were reported.

It should be noted that, in recent years, scaffolds are recognized as an alternative material with porous structure for advanced applications, such as bioactive molecule delivery, medical implants, cultured artificial organs, and tissue

engineering.[8-12] Until now, the techniques known for preparing scaffold are, for example, polymer assembly, phase separation, and electrospinning. The polymer assembly is a preformed structure based on the molecular interactions, such as hydrophilic, hydrophobic, and ionic interactions, etc. Fields et al.[13] reported the preparation of the collagen-like scaffold based on an assembly of peptide-amphiphiles connecting with mono- or di-alkyl ester lipid. The phase separation technique deals with a three dimensional continuous fibrous network, after lyophilizing the aqueous polymer solution.[14-15] Electrospinning is another technique practical to many types of polymers in the solution state. The precipitation of micro/nanofiber under electric potential gives an effective scaffold structure. For chitosan, phase separation[15] and electrospinning[16] techniques to initiate the chitosan scaffold using chitosan solutions or the cross-linked chitosan gels have been reported. Park et al.[17] and Li et al.[18] demonstrated that the conjugation with bioactive molecules, such as galactose and fructose, onto a chitosan scaffold increased the hepatocytes adhesion.

In recent years, nanomaterials have received much attention due to a good understanding of the relationship between the chemical structures, the packing structures and morphologies, and the induced properties. For a scaffold with nanoscaled matrices, we basically expect high surface area, regular pore size, and a well-defined pore structure. The target of nanoscaffold chemistry includes not only the mimicry of extra-cellular nanoscaled matrices but also the conjugation with bioactive molecules for an effective cell adhesion.

Considering that the chitosan scaffold satisfies the conditions for resorbable materials used in tissue engineering, further development in this field might be related to ways to initiate the nanoporous structure in the scaffold and modify it with bioactive molecules to achieve high surface area together with enhancement of specific cell adhesion and/or proliferation. From this viewpoint, the present work demonstrates a simple but effective way to obtain a novel soft and cotton-like chitosan nanoscaffold with disaccharide molecules conjugated on the surface. In our expectation, the material obtained might not show toxicity, as all preparation steps are in aqueous states and the conjugated functional group is sugar.

Experimental

Materials. Chitin flakes from shrimp shells were provided by Seafresh Chitosan (Lab) Company Limited (Bangkok, Thailand). Lactose monohydrate, maltose monohydrate, and sodiumcyanohydridoborate ($NaBH_3CN$) were purchased from Wako (Osaka, Japan). Sodium hydroxide, sodium chloride, hydrochloric acid, and acetic acid were obtained from Lab-Scan (Stillorgan, Ireland). Hexafluoro-2-propanol (HFP) was provided by Central Glass Co., Ltd. (Tokyo, Japan). Sodium trifluoroacetate (CF_3CO_2Na) was purchased from TCI-EP (Tokyo, Japan). All chemicals were analytical grade and were used without further purification.

Instruments and Equipment. Qualitative and quantitative Fourier transform infrared spectra were obtained from a Thermo Nicolet Nexus 670 (Madison, USA) with 32 scans at a resolution of 2 cm^{-1}. A frequency range of 4000-400 cm^{-1} was observed using a deuterated triglycinesulfate detector with a specific detectivity, D^*, of 1×10^9 cm $Hz^{½}$ w^{-1}. Wide angle X-ray diffraction (WAXD) patterns were recorded over 2-60° 2θ by a RIGAKU RINT 2000 (Tokyo, Japan) using CuKα as an X-ray source equipped with Ni filter with operating conditions of 40 kV and 30 mA. Thermogravimetric analyses were carried out using a Perkin Elmer Pyris Diamond TG-DTA (Connecticut, USA) with N_2 flow rate of 20 mL/min and a heating rate of 10°C/min starting from 30 to 650°C. ^1H NMR spectrum was recorded for the samples dissolved in CD_3COOD/D_2O on a JNM-A500 500 MHz spectrometer (Tokyo, Japan) at 70°C. The morphology of whisker was investigated by a JEOL JEM-1230 transmission electron microscope (TEM) (Tokyo, Japan) at 80 kV, and a JEOL JSM-5200 scanning electron microscope (SEM) (Tokyo, Japan) at 15 kV. Surface area was measured by a Quantachrome Corporation Autosorb-1 gas sorption analyzer (Florida, USA) via the Brunauer-Emmett-Teller (BET) method. Nitrogen gas was applied to calibrate the analyzer and was used as the adsorbate at liquid nitrogen temperature. The samples were degassed at 100°C overnight before measurement. Molecular weight was measured by a Tohso HLC-8220 gel permeation chromatograph (GPC) (Tokyo, Japan), equipped with RI detector and Tohso TSK-gel super H-RC and HM-N columns, and the operating temperature was

40°C. HFP containing 10 m*M* CF_3CO_2Na was used as an eluent with a flow rate of 0.2 mL/min and polymethyl methacrylate was used as a standard.

Procedures.

Preparation of chitin whisker, 2. Chitin flakes, **1** (1.00 g), were treated in 3 *N* hydrochloric acid (HCl) (100 mL) and stirred at reflux for 3 h before centrifugation. The treatment with 3 *N* HCl was repeated three times. Finally, the residues were collected and dialyzed in distilled water until neutral to obtain chitin whiskers, **2**, for 86% yield (Scheme 5.1).

FT-IR (KBr, cm^{-1}): 1661, 1624, and 1557 cm^{-1} (amide I and amide II).

Preparation of chitosan nanoscaffold, 3. Compound **2** (20 mL) was stirred in NaOH aq. (40% w/v 100 mL) at reflux for 7 h before leaving at room temperature overnight. The treatment with 40% NaOH aq. was repeated two times. The crude product was dialyzed till neutral in distilled water to obtain **3** for 92% yield (Scheme 5.1).

FT-IR (KBr, cm^{-1}): 1595 cm^{-1} ($-NH_2-$). ^1H NMR (δ, ppm): 2.367 (NHAc), 3.435 (H2 of GlcN unit in chitosan), 4.023-4.255 (H2 of GlcNAc, and H3-H6 of pyranose ring), 4.9 (H1 of GlcNAc), 5.138 (H1 of GlcN).

Preparation of chitosan nanoscaffold conjugated lactose, 4. Compound **3** (0.03 g in 5.0 mL) was suspended in NaCl solution (1.0 *M*, 10 mL). Lactose monohydrate (0.224 g, 3 moles equivalent to pyranose rings) and $NaBH_3CN$ (0.039 g, 3 moles equivalent to pyranose rings) were added with a catalytic amount of acetic acid to the suspension of **3**. The reaction was carried out at room temperature for 3 days. The crude product was purified by dialyzing in distilled water and was lyophilized to obtain **4** in 87.6% yield (Scheme 5.1). The degree of substitution was 9.5%.

FT-IR (KBr, cm^{-1}): 1530 cm^{-1} ($-NH-CH_2-$). ^1H NMR (δ, ppm): 2.414 (NHAc), 3.527 (H2 of GlcN unit in chitosan), 3.554-4.431 ($-NH-CH_2-$, H2 of GlcNAc, H3-H6 of pyranose ring, and H2', H3', H4', H5', H6', H2", H3", H4", H5", H6" substituted), 4.907-4.932 (H1 of GlcNAc), 5.203-5.230 (H1 of GlcN).

Preparation of chitosan nanoscaffold conjugated maltose, 5. Compound **5** was prepared similar to **4** but using maltose monohydrate and obtained 72.1 % yield (Scheme 5.1). The degree of substitution was 7.3%.

FT-IR (KBr, cm^{-1}): 1530 cm^{-1} (-NH-CH_2-). ^1H NMR (δ, ppm): 2.410 (NHAc), 3.519 (H2 of GlcN unit in chitosan), 3.723-4.442 (-NH-CH_2-, H2 of GlcNAc, H3-H6 of pyranose ring, and H2', H3', H4', H5', H6', H2", H3", H4", H5", H6" substituted), 4.902-4.927 (H1 of GlcNAc), 5.197-5.224 (H1 of GlcN).

Scheme 5.1

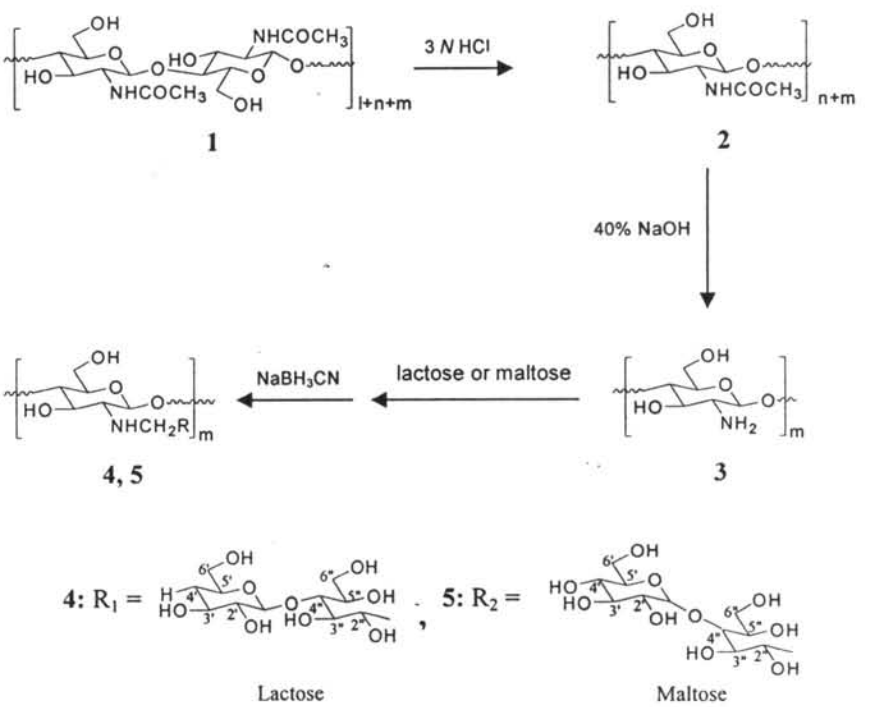

Degree of deacetyiation.[19] Degree of deacetylation (DD) of **3** was calculated by Eq. (1) based on ^1H NMR spectrum. The peaks in consideration were the one at 2.376 ppm (*N*-acetyl group) and the broad one at 4.023-4.255 ppm (pyranose ring).

$$DD\ (\%) = \{1 - [(I_{CH_3} / 3) / (I_{\text{pyranose ring}} / 6)]\} \times 100\% \quad (1)$$

Degree of substitution.[20] The degree of substitution (DS) was calculated by Eq. (2) using the peaks of the substituted group and the pyranose ring appearing at 3.50-4.51 ppm.

$$DS\ (\%) = (I_{NHCH_2} - 6)/14 \times 100\% \quad (2)$$

Results and Discussion

Chitin Whisker, 2

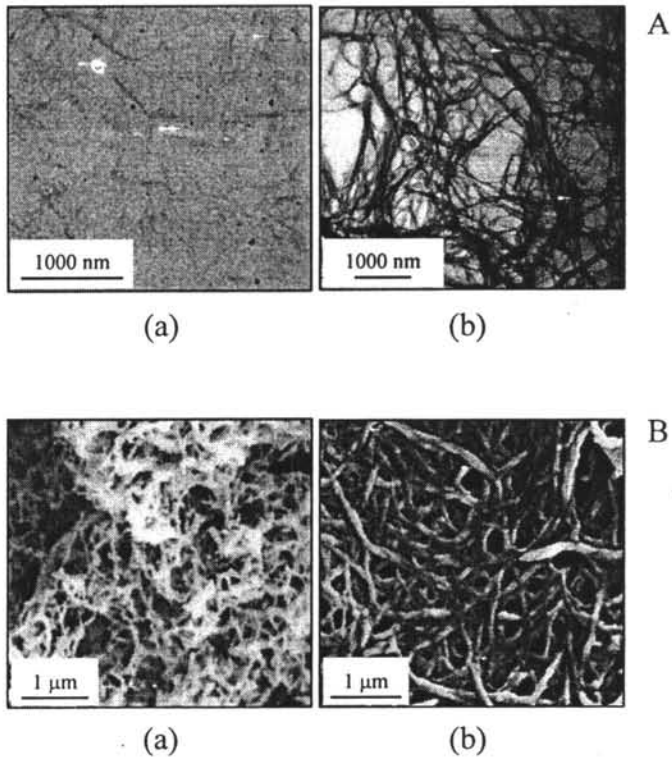

FIGURE 5.1 TEM micrographs of (A) (a) **2** and (d) **3** and SEM micrographs (B) (a) **2** (× 20,000) and (b) **3** (× 20,000).

When the chitin flakes were treated in 3 *N* HCl for 3 h, the colloidal solution was obtained. Previously, Nair et al.[21] demonstrated that the product was in a uniform whisker morphology, as observed by TEM. In our case, similar procedures were carried out but without the steps of antibacterial reagent addition and storage in aqueous at pH 4 as we continuously carried out the deacetylation. After the colloidal

solution was obtained, the solution was lyophilized to obtain **2**. The FT-IR confirmed that **2** remained in the structure of chitin with the characteristic peaks at 1661, 1624, and 1557 cm^{-1} (amide I and amide II). The TEM micrograph clarifies that **2** is in whisker structure with a length of 200-560 nm and a width of 18-40 nm to result in the average aspect ratio of 18 (Figure 5.1A (a)).

In general, the treatment with acid brings about the depolymerization. Here, GPC was used to determine the molecular weight of chitin whisker using HFP as the solvent, as reported by Sashiwa et al.[22] The molecular weight of chitin whisker was found to be 62,838 Da, whereas that of the starting chitin was 2,174,281 Da. This confirms the depolymerization of chitin when its morphology changed to whisker.

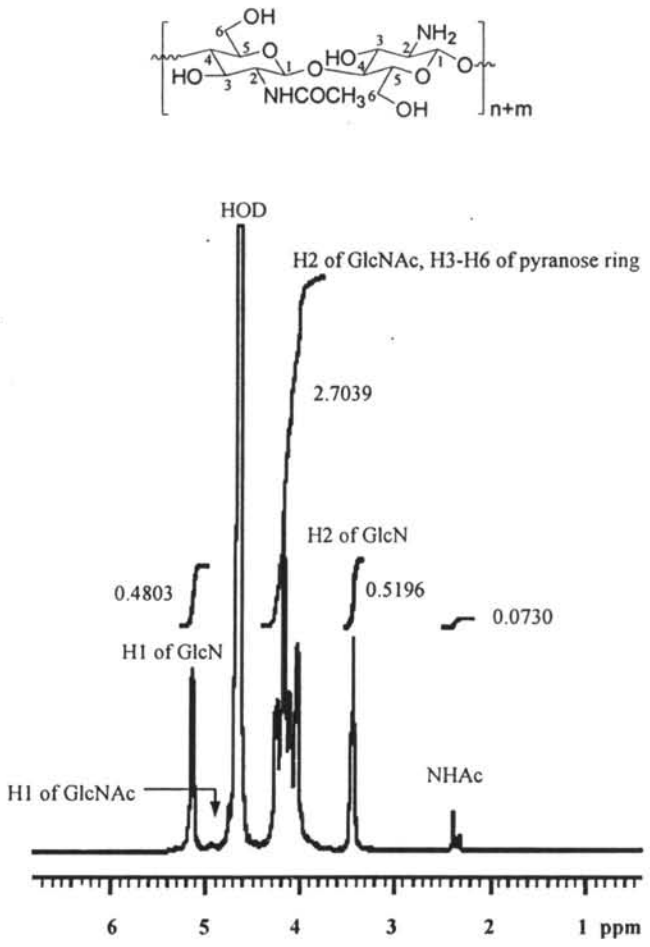

FIGURE 5.2 ^{1}H NMR spectrum of **3.**

Chitosan Nanoscaffold, 3

Compound **2** was treated with a high concentration of NaOH solution for three days at reflux to find that the solution was still in a milky colloidal state. The colloidal solution was lyophilized to obtain **3**. The FT-IR spectrum of **3** showed that the compound was chitosan, based on the significant decrease in peaks at 1661, 1624, and 1557 cm^{-1} (amide I and amide II), and a new peak at 1595 cm^{-1} ($-NH_2$). The ^1H NMR spectrum exhibits the chitosan peaks, of which the degree of deacetylation is 95% (Figure 5.2). Based on the fact that **3** was prepared from the nanosized whisker of **2**, and appeared as a colloidal solution without precipitation, we expected to see **3** in any forms of nanosized particles. From the TEM and SEM observations, surprisingly, **3** (Figure 5.1A (b) and 5.1B (b)) shows a network structure which is completely different from the whisker appearance of **2**. Figure 5.1A (b) clarifies that each fiber is connected to each other and swelling or crossing to other fibers to result in the matrices or scaffold. On average, the thickness of the fibers is 40 ± 10 nm. It should be noted that when **2** was deacetylated to **3**, the crystallinity was gradually reduced and the branching of chitosan became significant. As a result, the nanoscaffold network could be observed (Figure 5.1A (b) and 5.1B (b)).

It is important to note that after **2** and **3** were lyophilized to prepare the samples for SEM, another level of morphology was identified. For **2**, the packing of nanosized whisker resulted in a fibrous aggregation and each fiber thickness was around 70 ± 20 nm (Figure 5.1B (a)). When it came to **3**, each of the fibers was packed and the fiber thickness was increased significantly to 120 ± 30 nm (Figure 5.1B (b)) to form a network with a pore diameter of 220 ± 30 nm.

Comparing the traditional treatment of chitin flakes to chitosan powder, the treatment of chitin whisker provides chitosan in nanoparticles form as can be observed easily from the colloidal state. As shown here, our further analysis confirmed that those nanoparticles are in the form of nanoscaffold.

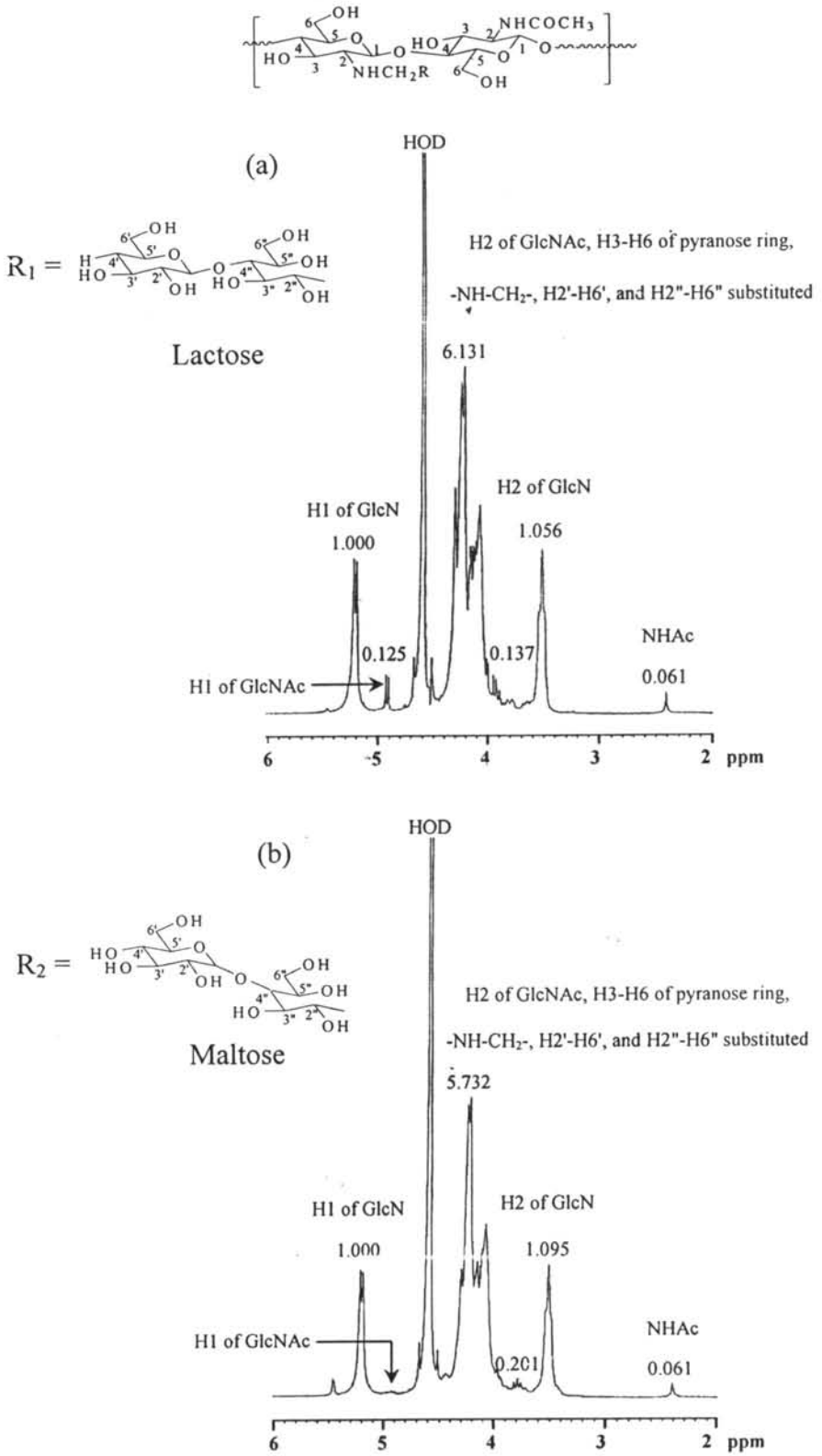

FIGURE 5.3 ^{1}H NMR spectra of (a) **4** and (b) **5**.

Conjugation of Lactose and Maltose

In the past, Sashiwa and Shigemasa[20] proposed water soluble chitosan derivatives by conjugating sugar units, such as lactose, fructose, and maltose onto chitosan via a homogenous system of lactic acid solution to achieve the degree of substitution at 44%. From this viewpoint, we considered the surface modification of **3** with maltose and lactose to propose a way to develop cell adhesion.

To initiate an aldehyde terminal to disaccharide, acid hydrolysis is required. However, as **3** dissolved well in aqueous acids, stabilization of the colloidal solution of **3** was needed. It was found that after adding NaCl to the colloidal solution of **3**, the solution was maintained in the colloidal state, even when an amount of acetic acid was further added. This might be due to the fact that an increase in ionic strength from NaCl obstructs the solubility of **3** in acid. As a result, the introduction of lactose and maltose onto **3** could be achieved in a heterogeneous system. Although the structural characterization by FT-IR is simple and easy, the fact that the disaccharide peaks overlap with the polysaccharide peaks of chitosan makes it possible to observe only the changes of the amino group. FT-IR spectra of **4** and **5** showed that the amino group of **3** was consumed after the reaction, as evidenced from the disappearance of the peak at 1595 cm^{-1} ($-NH_2$, -N-H- in plane bending). A new peak at 1530 cm^{-1} ($-NH-CH_2-$, -N-H- in plane bending) also confirmed the conjugation of lactose and maltose via the amino group of chitosan, or in other words, the success of **4** and **5**. ^1H NMR was applied to identify the structure and degree of substitution of chitosan with the consideration on the overlap of saccharide peaks belonging to disaccharide and chitosan units (Figure 5.3 a and b). Based on Eq. (2), the degrees of substitution of **4** and **5** were found to be 9.5 and 7.3%, respectively.

Soft and Cotton-like Chitosan-Sugar nanoscaffold

Compound **2** shows peaks at 9° 2θ and 19° 2θ, whereas **3** exhibits significant broad peaks at 10, 20 and 22° 2θ (Figure 5.4 a and b). After disaccharide conjugation, **4** and **5** show significant broad peaks at 10, and 20° 2θ (Figure 5.4 c and d). This implies the loose packing structure of **3** as a result of the introduction of a bulky sugar unit.

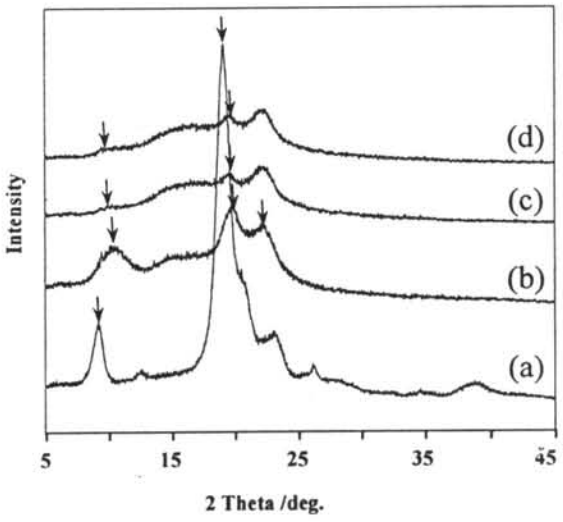

FIGURE 5.4 WAXD patterns of (a) **2**, (b) **3**, (c) **4**, and (d) **5**.

TEM was applied to observe the structures of **4** and **5.** Figure 5.5 a and b show that both are in nanoscaled scaffold, similar to **3.** The average thickness of each fiber in nanoscaffold was 10-15 nm. The average thickness of these fibers was smaller than that of **3**, implying that the modification with sugar initiates the separation of the original fibrous network of **3**. This might be due to the introduction of lactose and maltose obstructing the packing of **3**.

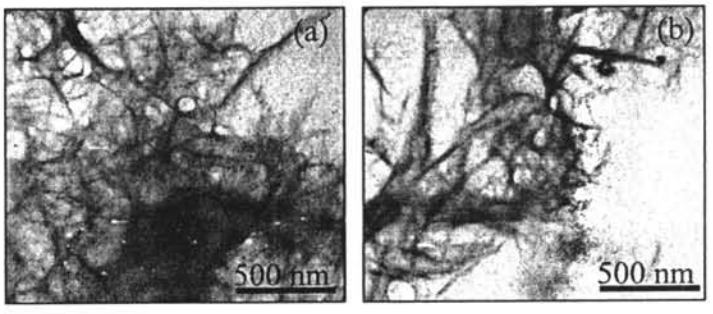

FIGURE 5.5 TEM micrographs of (a) **4** and (b) **5**.

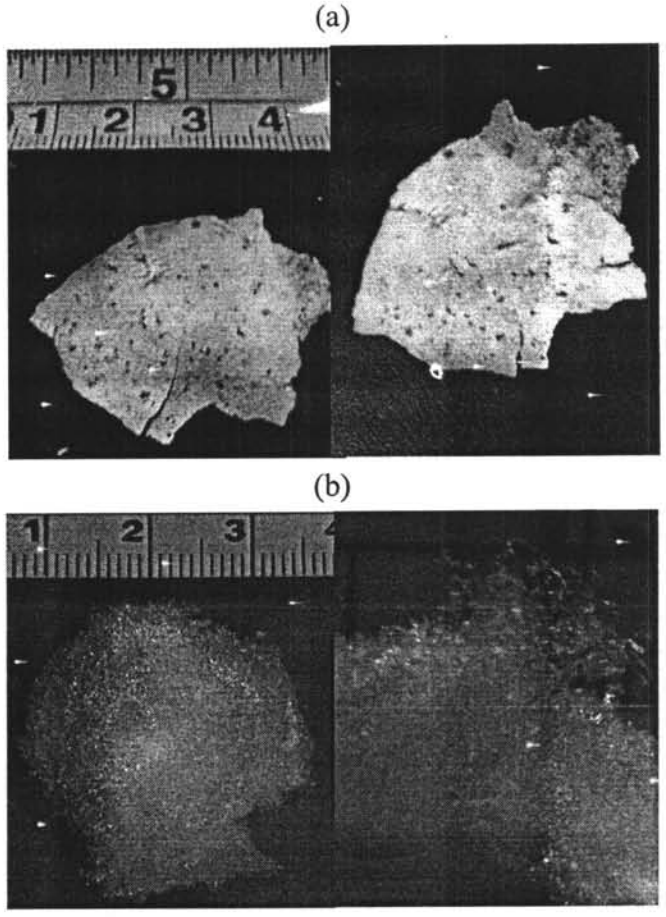

FIGURE 5.6 Appearances of (a) **3** and (b) **4** after lyophilization.

Similar to **3**, the lyophilization of the colloidal solution might bring about the scaffold aggregation. For **3**, the appearance was a flat white soft porous sheet (Figure 5.6a). It is important to mention that, after **4** and **5** were lyophilized; the morphology was changed totally. Both exhibited glossy soft and cotton-like appearance consisting of tiny fibers. Figure 5.6b is an example of this glossy soft and cotton-like appearance of **4**. The size and shape of these cotton-like materials could be easily controlled by the mold while lyophilizing. When a few drops of water were added, each fine fiber was aggregates. Observation by SEM clearly shows that **4** and **5** exhibit quite a unique morphology under the three dimensional mesoporous network (Figure 5.7 a and c). By focusing on some particular area of **4** and **5**, the flat mesoporous networks were also identified (Figure 5.7 b and d) with an average pore diameter of 27 ± 3 μm. The solubility was studied to find that **4** and **5** were also as

well dissolved in acetic acid as **3**, but swelled in polar solvents such as methanol and ethanol including chloroform.

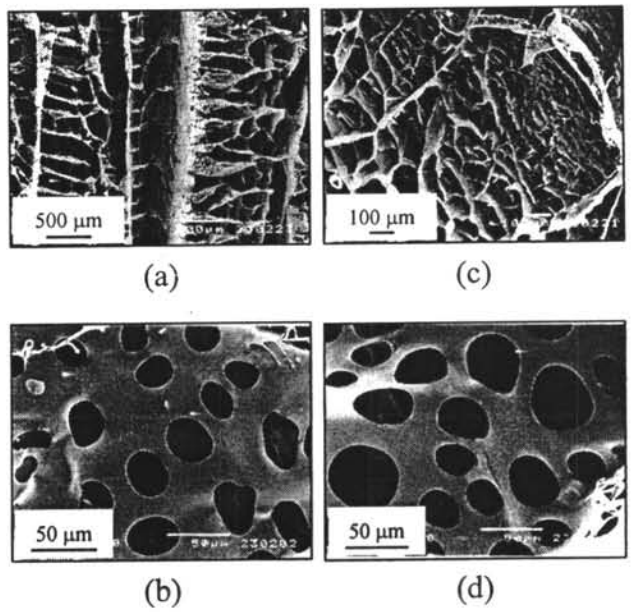

FIGURE 5.7 SEM micrographs at 15 kV of (a) **4** (× 35), (b) **4** (× 500), (c) **5** (× 100), and (d) **5** (× 500).

Table 5.1 summarizes how the functionalization with lactose and maltose affects the thermal stability. The degradation temperature (T_d) of **2** is 387°C whereas that of **3** is 308°C. The decrease in degradation temperature when chitin is deacetylated to chitosan is known as a result of the looseness in the packing structure based on the changes in inter- and intramolecular hydrogen bond pattern.[23]

Table 5.1 Degradation temperature (T_d) and surface area of **2**, **3**, **4**, and **5**

Compound	T_d (°C)	Surface area(m^2/g)
2	387	18.44 ± 14.46
3	308	64.70 ± 14.26
4	259	97.12 ± 38.91
5	263	87.80± 18.86

The degradation temperatures of **4** and **5** decreased significantly to be at 260°C and 263°C, respectively, compared to that of **3**. This suggests the looseness in the chain packing after introducing sugar units.

BET measurement was applied to evaluate the surface areas of **2-5** (Table 5.1). Compound **2** gave a surface area of 18.44 ± 14.46 m^2/g whereas **3** exhibited it for up to 3.5 times that of **2**. The increase in surface area of **3** supported its morphology as was clarified in SEM micrographs (Figures 5.1B (a) and (b)). For **4** and **5**, as expected, the surface areas were increased significantly (more than 1.5 times) compared to that of **3**. This reflected the loose packing structure of **3** after conjugating with sugar units and supported the soft and cotton-like appearance

Conclusions

Chitosan nanoscaffold was successfully obtained by deacetylating chitin whisker. The nanoscaffold offered an effective reaction to conjugate the maltose and lactose in a heterogeneous system at room temperature. After maltose or lactose was conjugated, the material exhibited beautiful glossy tiny cotton ball fibers. SEM and TEM micrographs revealed that the materials obtained were in nanoscaffold structure with mesopores. The preparations of chitosan nanoscaffold and chitosan-sugar nanoscaffold were accomplished in water to result in organic solvent free biomaterials. Our studies on cell adhesion of these chitosan-sugar nanoscaffolds are in progress.

Acknowledgements

The authors gratefully acknowledge the partial financial support from the Royal Golden Jubilee Ph. D. Program, the Thailand Research Fund, and the National Research Council of Thailand (NRC 12/2548). One of the authors (S.C.) is indebted to the generous contribution of the Hitachi Scholarship Foundation to the continuation of his research activities. The authors extend their appreciation to the Seafresh Chitosan (Lab) Company Limited, Thailand for the chitosan material.

References

1. Dumitriu, S.; Popa, M. I.; Cringu, A.; Stratone, A. Colloid and Polymer Science 1989, 267, 595-599.
2. Singh, D. K.; Ray, A. R. J Appl Polym Sci 1994, 53, 1115-1121.
3. Yamamoto, H; Amaike, M. Macromolecules 1997, 30, 3936-3937.
4. Chandy, T.; Sharma, C. P. Biomaterials 1992, 13, 949-952.
5. Bégin, A.; Calsteren, M. R. V. Inter J Bio Macromol 1999, 26, 63-67.
6. Hoagland, P. D.; Parris, N. Ind Eng Chem Res 1997, 36, 3631-3638.
7. Zeng, X.; Ruckenstein, E. Ind Eng Chem Res 1996, 35, 4169-4175.
8. Mao, J. S.; Liu, H. F.; Yin, Y.; Yao, K. D. Biomaterials 2003, 24, 1621-1629.
9. Davis, M. W.; Vaccanti, J. P. Biomaterials 1996, 17, 365-372.
10. Khor, E.; Lim, L. Y. Biomaterials 2003, 24, 2339-2349.
11. Ma, J.; Wang, H.; He, B.; Chen, J. Biomaterials 2001, 22, 331-336.
12. Yin, Y.; Ye, F.; Cui, J.; Zhang, F.; Li, X.; Yao, K. J Biomed Mater Res A 2003, 67, 844-855.
13. Fields, G. B.; Lauer, J. L.; Dori, Y.; Forns, P.; Yu, Y. C.; Tirrell, M. Biopolymers 1998, 47, 143-147.
14. Smith, L. A.; Ma, P. X. Colloid Surface B 2004, 39, 125-131.
15. Madihally, S. V.; Matthew, H. W. T. Biomaterials 1999, 20, 1133-1142.
16. Bhattarai, N.; Edmonson, D.; Veiseh, O.; Matsen, F. A.; Zhang, M. Biomaterials 2005, 26, 6176-6184.
17. Park, I. K.; Yang, J.; Jeong, H. J.; Bom, H. S.; Harada, I.; Akaike, T.; Kim, S. I.; Cho, C. S. Biomaterials 2003, 24, 2331-2337.
18. Li, J.; Pan, J.; Zhang, L.; Yu, Y. Biomaterials 2003, 24, 2317-2322.
19. Lavertu, M.; Xia, Z.; Serreqi, A. N.; Berrada, M.; Rodrigues, A.; Wang, D.; Buschmann, M. D.; Gupta, A. J Pharmaceut Biomed 2003, 32, 1149-1158.
20. Sashiwa, H.; Shigemasa, Y. Cabohyd Polym 1999, 39, 127-138.
21. Nair, K. G.; Dufresne, A. Biomacromolecules 2003, 4, 666-674.
22. Sashiwa, H.; Kawasaki, N.; Nakayama, A.; Muraki, E.; Aiba, S. Chitin and chitosan research 2002, 8, 249-251.
23. Kittur, F. S.; Harish Prashanth, K. V.; Udaya Sankar, K.; Tharanathan, R. N. Cabohyd Polym 2002, 49,185-193.